Colloid and Polymer Science (2022) 300:1049–1062
https://doi.org/10.1007/s00396-022-05007-8

ORIGINAL CONTRIBUTION

Ion partitioning and ion size effects on streaming field and energy conversion efficiency in a soft nanochannel

Dipankar Kundu[1] · S. Bhattacharyya[1] · Partha P. Gopmandal[2]

Received: 30 March 2022 / Revised: 5 June 2022 / Accepted: 27 June 2022 / Published online: 25 July 2022

Abstract
Numerical modeling on streaming field and electroviscous effect in a soft nanochannel is made by considering the finite ion size and ion partitioning effects. The standard electrokinetic model is modified by incorporating the finite ion size effect and the effect of ion partitioning, which arises due to the difference in dielectric permittivity between the electrolyte and wall grafted polyelectrolyte layer (PEL). Such modification in the ion transport equations enable us to consider higher range of wall charge density as well as higher volumetric charge density of the PEL. The dielectric permittivity of the PEL may become lower due to the large accumulation of counterions drawn by the PEL immobile charges. The ion steric repulsion is taken into account through the BMCSL (Boublik-Mansoori-Carnahan-Starling-Leland) equation based on the hard-sphere model of ions. This enables to consider different ion sizes, which arise when a mixture of different salts is considered. The governing equations are solved numerically and the streaming field is determined iteratively. We find that the ion steric interactions and ion partitioning effects create a counterion saturation. This leads to a reduction in the counterion condensation of the PEL when the PEL and wall are similarly charged, which results in higher streaming field and energy conversion efficiency. The diffuse PEL of pore size in the order of the channel half height creates higher energy efficiency compared to the channel consisting of rigid walls.

Keywords Soft nanochannel · Diffuse polymer layer · Streaming potential · Ion size effect · Ion partitioning effect · Numerical method

Introduction

When a charged surface is in contact with an electrolyte medium an electric double layer (EDL) with surplus counterions (ions of opposite polarity to the surface charge) develops at the surface-liquid interface. A pressure-driven flow of the electrolyte above the charged surface convects the mobile ions in EDL downstream and an electric current, referred to as the steaming current, along the direction of the fluid flow develops. The accumulation of ions in the downstream governs an electric field, the streaming field, which creates a conduction current along the opposite direction to the fluid flow. At a steady state the conduction current becomes equal to the streaming current (or convection current) so as to satisfy an overall zero electric current in absence of an externally imposed electric field. The streaming field generates an electroosmotic flow (EOF) of the electrolyte opposing the pressure-driven flow. This diminished pressure-driven flow due to the steaming potential can be conceptualized as an increment in the electrolyte effective viscosity, the electroviscous effect (EVE). The experimental results of van der Heyden et al. [1] for the streaming current in a pressure-driven liquid flow through a single nanochannel shows a linear relation between the pressure gradient and streaming current.

The streaming current can be supplied to the external load resistor to achieve the electrical power from the hydrodynamic energy. Therefore, generation of streaming current provides a mechanism of converting mechanical work into electrical power [2]. The streaming potential measurement is the most widely used technique for determining the ζ-potential of membranes [3]. Streaming potential generation and

✉ Partha P. Gopmandal
partha.gopmandal@maths.nitdgp.ac.in;
parthap1218@gmail.com

[1] Department of Mathematics, Indian Institute of Technology Kharagpur, Kharagpur 721302, India

[2] Department of Mathematics, National Institute of Technology Durgapur, Durgapur 713209, India

the electroviscous phenomena have several other applications such as sorting of nanoparticles, dispersion and separation of DNA molecules and so on [4, 5]. Substantial progress is made on the generation of streaming potential (SP), associated EVE and conversion of the hydraulic power to electrical power by means of pressure-driven flow across the slit-like microfluidic devices [5–10].

The streaming current due to the pressure-driven flow in a microchannel is of the order of a nano ampere [11]. In recent, years several attempts are made to improve the energy conversion efficiency in a single microchannel. In order to improve the efficiency several authors studied the SP and EVE effect in soft microchannels [12–17]. The soft microchannel is a typical engineered channel where the channel walls are grafted with soft polymeric material, the polyelectrolyte layer (PEL), that allows the penetration of electrolyte ions and liquid. The PELs entrap the additional immobile charges, which certainly changes the EDL electrostatics and thereby the electrokinetic transport of ionized liquid across the soft channels. Das and co-authors [18–21] studied extensively the SP, EVE and the SP-induced energy conversion in a soft nanochannel by considering step-like PEL. The diffuse description of PEL, which is characterized by the decay length, is however more realistic and it can consider the impact of swelling of the soft layer. It is noteworthy to mention here that the diffuse soft PEL avoids the need to specify any interfacial boundary conditions across the PEL-to-electrolyte interface. Duval et al. [22, 23] studied the generation of SP through soft nanochannel considering the diffuse distribution of monomers and immobile charges across the PEL.

In all the aforementioned studies on the generation of SP, EVE and energy conservation in soft nanochannel, the dielectric permittivity of the PEL and electrolyte is assumed to be the same, which is however possible for dilute polymer system [24]. In general, the dielectric constant of the sufficiently dense PELs is lower than that of the aqueous medium [25–27]. For membrane materials, the dielectric permittivity is lower than that of the aqueous medium [28]. This difference in dielectric constant between two medium leads to a difference in electrostatic free energy or Born energy of ions in both the phases [29]. The ion gains Born energy when it moves from a region of high dielectric permittivity to a region of low dielectric permittivity. As a result, the penetration of mobile ions in the PEL revises, which is referred to as ion partitioning effect. Recently Poddar et al. [30] studied the impact of ion partitioning on the generation of SP and EVE in a soft nanochannel by considering a step-like PEL.

The transport of ions is modeled by adopting the standard mean-field theory, e.g., Boltzmann distribution or Nernst-Planck equation, in which the electrolyte ions are considered to be effective point charges and neglect the short range ion-ion interactions. This consideration may lead to the possibility of sufficiently large accumulation of counterions near a moderate to highly charged surface immersed in aqueous solution. Monomers of fixed charge in the PEL attract mobile counterions within the PEL. For a highly charged PEL a large volume of mobile counterions is drawn in PEL leading to the relevance the ion steric interactions become important due to the presence of a large volume of mobile counterions. Bikerman [31] introduced the modified Boltzmann equation to account the volume exclusion due to ion steric repulsion in the ion distribution. Based on the Bikerman model the finite ion size effects on the streaming potential and electroviscous effect in the soft channel are analyzed by Koranlou et al. [32] and Xing and Jian [33]. These studies show that the volume exclusion due to ion steric repulsion amplifies the electrical potential in the soft channel. The ion transport due to convection and diffusion is important in the pressure-driven flow within a microchannel. These effects are ignored when Boltzmann distribution of ions is considered. In addition, for the nanochannel in which Debye length is in the order of the length scale, the Bikerman model is not effective.

Carnahan and Starling [34] model based on the hard-sphere fluid theory for ion steric repulsion has the larger range of volume fraction and desirable accuracy among several other models [35, 36]. Further extension of this model, the Boublik-Mansoori-Carnahan-Starling-Leland (BMCSL) model [37], is applicable for ionic species with unequal sizes. Several authors [38–40] studied the electrokinetics near a charge surface immersed in mixed electrolyte solution of different sizes of hydrated ions by adopting the BMCSL model. However, none of the existing study on streaming potential has analyzed the finite ion size effects based on the BMCSL model. The modified Nernst-Planck equation with the BMCSL model to incorporate the finite ion size effects is more appropriate than the Boltzmann-Bikerman equation to analyze the pressure-driven flow of electrolyte in slit micro or nanochannels. In addition, the BMCSL model can handle mixture of different ionic species.

In this paper impact of the finite ion size effect and PEL-to-electrolyte dielectric permittivity ratio on electrokinetic energy harvesting in a soft nanochannel is analyzed. The soft channel is comprised of a charged polyacrylamide hydrogel film (PEL) supported by charged rigid surface consisting of Teflon AF [22]. We have considered the modified Nernst-Planck equation for ion transport, which incorporates ion steric repulsion and ion partitioning due to the difference in dielectric permittivity between the PEL and electrolyte solution. The PEL-to-electrolyte dielectric permittivity ratio creates a Born energy difference in ions, which leads to an ion partitioning effect. Consideration of ion steric effect and ion partitioning effect on electrokinetics in the soft nanochannel is relevant when the highly charged PEL and/or higher surface charge density of the channel walls is considered. The

present study reveals a significant improvement in streaming potential mediated energy conversion in a soft channel with diffuse PEL of high permeability and lower dielectric permittivity. The ion saturation due to volume exclusion of ions and ion partitioning have a significant impact on the streaming field and EVE.

Mathematical model

We consider the generation of SP and EVE in a slit soft nanochannel by creating a pressure-driven flow of an electrolyte solution with bulk concentration $\bar{c_0}$. The electrolyte is composed of binary or valence asymmetric ions with valence z_i and concentration c_i. A constant axial pressure gradient is applied along the axis of the channel (Fig. 1). The channel height ($2h$) is taken to be much greater than the width of the channel. Here width refers to the extension of the system perpendicular to the plane of Fig. 1. Such a consideration allows us to consider the flow to be two-dimensional. The channel walls bearing a uniform surface charge density σ are coated with diffuse PEL of fixed volumetric charge density $\rho_{fix} = zFN$, where F is the Faraday constant and z, and N are the valence and molar concentration of fixed charges residing in PEL, respectively. The distribution of the polymer segment within the diffuse PEL is given by [22]

$$f(y) = w\left[1 - \tanh\left\{\frac{(h-y)-d}{\alpha}\right\}\right] \tag{1}$$

where α is the characteristic decay length, which defines the diffuse nature of the soft PEL. For $\alpha = 0$, the polymer segments are uniformly distributed and such a description of the PEL termed as step-like PEL with nominal thickness d. It may be noted that for nonzero values of α, the thickness of the PEL extends beyond the nominal thickness (d) and an estimate for the diffuse PEL thickness becomes $\bar{d} = d + 2.3\alpha$ [22, 41]. Here we consider the thickness of the diffuse PEL lower than the channel half height, i.e., $\bar{d} < h$ to avoid the overlapping of the adjacent PELs grafted on the bounding walls of the channel. The parameter w appearing in Eq. (1) ensures a fixed amount of polymer segments across the PEL while varying the decay length [22] and is given by

$$w = \frac{d}{\alpha \log\left(1 + e^{2d/\alpha}\right)} \tag{2}$$

For a diffuse soft PEL, the inverse of Brinkmann screening length $\ell(y)$ can be expressed as

$$\ell(y) = \ell_0\sqrt{f(y)} \tag{3}$$

Here, ℓ_0^{-1} is the Brinkmann screening length for a step-like PEL for which $\alpha \to 0$.

The dielectric permittivity of the PEL is generally lower than that of the bulk aqueous medium, which leads to a nonzero difference in electrostatic free energy or Born energy ΔW_i of the i^{th} ionic species between the two mediums [42]. The Born energy [29] defined as the electrostatic energy required to transfer an ion from a vacuum to a dielectric medium. This Born energy difference leads to an ion partitioning effect, which modify the ion transport at the PEL-electrolyte interface. If we denote f_i (i=1,2,..N) as the ion partitioning coefficient of the i^{th} ionic species then the ion concentration in PEL modifies to $c_i f_i$ and hence, the modified net charge due to mobile ions within the PEL is given by $\bar{\rho}_e = \sum_{i=1}^{N} F z_i \bar{c}_i f_i$. Here the ion partitioning coefficient of the i^{th} electrolyte ion is given by $f_i = \exp(-\Delta W_i/k_B T)$ [26, 27, 30, 42], where

$$\Delta W_i = \frac{(z_i e)^2}{8\pi r_i}\left(\frac{1}{\epsilon_p} - \frac{1}{\epsilon_e}\right) \tag{4}$$

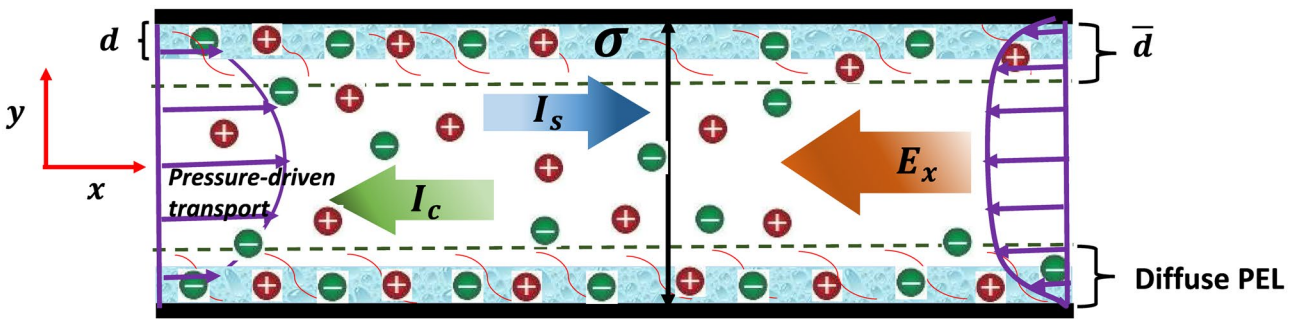

Fig. 1 Schematic of the present situation for the generation of streaming potential under applied pressure gradient. The lower and upper walls are charged with constant surface charge density σ. The surface of the solid plates is covered with an ion penetrable charged diffuse polyelectrolyte layer (PEL) bearing volumetric charge density ρ_{fix}

Here r_i is the radius of ion with valence z_i and e is the elementary charge. The dielectric permittivity of the PEL and the bulk electrolyte are ϵ_p and ϵ_e, respectively. In this model we have considered constant dielectric permittivity for the electrolyte medium and PEL with a step-change in permittivity at the PEL-electrolyte interface. Thus, the ion-solvent interaction arises at the interface between the PEL and electrolyte, where the ion transport is affected by the Born energy difference. By virtue of Eq. (4), the ion partitioning coefficient depends on the ion size; however, the medium permittivity is considered to be invariant due to the variation of ion concentration. As the ions are considered to be of finite size, the volume exclusion effect due to ion-ion steric interactions is included in the present analysis. However, the ion-solvent interactions which lead to a spatially variant dielectric permittivity of the medium and viscosity are not taken into account.

It may be noted that the hydrated ions lower the medium permittivity by forming hydration shell around the ion. In that case the medium permittivity varies with the ionic concentration and hence, permittivity becomes a spatially varying quantity. This phenomena which leads to the ion-solvent interactions is termed as the dielectric decrement [43–45]. The ionic concentration at any location is influenced by the steric repulsion of hydrated ions. Thus, ion steric interactions can influence the permittivity of the medium. The dielectric decrement creates a further counterion saturation by decreasing the permittivity of the medium. In the present model we have neglected the impact of dielectric decrement, which could be justified for the low to moderate range of electrolyte concentration. However, the ion partitioning is significant when there is a step-change in permittivity at the PEL-electrolyte interface. In the present model we have considered the volume exclusion due to steric interactions of finite sized ions. The steric interactions near the highly charged channel wall and PEL can have significant impact even at a moderate range of bulk ionic concentration.

Owing to the symmetry about the central line $y = 0$ of the flow, we consider only the upper half of the channel. In order to consider the ion partitioning effect, we need to identify the region of PEL and the regions filled with electrolyte solution. To identify different regions in the flow domain, we introduced a binary constant A which is equal to 1 in the PEL, i.e., $h - \bar{d} \le y \le h$ where $f(y) \neq 0$ and it is equal to 0 for the range $0 \le y \le h - \bar{d}$ for which $f(y) = 0$ (in the electrolyte medium). The governing equations for the pressure-driven flow of the electrolyte within the soft nanochannel are the equation for electrostatic EDL potential, ion and fluid transport equations. The EDL potential is governed by the Poisson equation as

$$-\nabla.[\{\epsilon_e - A(\epsilon_e - \epsilon_p)\}\nabla\phi] = \sum_{i=1}^{N} F z_i \bar{c}_i f_i + \rho_{fix} f(y) \tag{5}$$

The transport of the i^{th} ionic species can be expressed based on the conservation of mass flux

$$\bar{\nabla}.\left[\bar{c}_i\bar{\mathbf{u}} - D_i\bar{\nabla}\bar{c}_i - \frac{D_i e z_i}{k_B T}\bar{c}_i\bar{\nabla}\bar{\phi} - D_i\bar{c}_i\bar{\nabla}\ln\nu_i\right] = 0 \tag{6}$$

where D_i, k_B and T are the diffusion coefficient of the i^{th} species, Boltzmann constant, absolute temperature, respectively and $\bar{\mathbf{u}} = (\bar{u}, \bar{v})$ is the velocity of the fluid. The first three terms inside the parentheses of Eq. (6) corresponds to the convective flux, diffusion flux, and electromigration flux, respectively. The fourth term arises due to the steric force for finite size of ions, which is however absent in standard Nernst-Planck equation for point-like ions. The activity coefficient ν_i can be expressed in terms of the local ionic volume concentration

$$\chi = (4\pi/3)N_A\sum_i r_i^3\bar{c}_i$$

The CS model provides $\nu_i = \exp(\chi(8 - 9\chi + 3\chi^2)/(1-\chi)^3)$. This model considers the same hydrated radius for both the cations and anions, which is the average of the cation and anion. The CS model can be extended to consider different ion sizes, which is considered in the BMCSL model [46]. In this model the activity coefficient is given by $\nu_i = \exp(\Upsilon_i)$, where Υ_i is the excess electrochemical potential of the ith ionic species due to the ion-ion interactions

$$\begin{aligned}\Upsilon_i = &-\left[1 + 2\left(\frac{\xi_2 r_i}{\chi}\right)^3 - 3\left(\frac{\xi_2 r_i}{\chi}\right)^2\right]\ln(1-\chi)\\ &+\frac{3\xi_2 r_i + 3\xi_1 r_i^2 + \xi_0 r_i^3}{1-\chi}\\ &+\frac{3\xi_2 r_i^2}{(1-\chi)^2}\left(\frac{\xi_2}{\chi} + \xi_1 r_i\right) - \xi_2^3 r_i^3\frac{\chi^2 - 5\chi + 2}{\chi^2(1-\chi)^3}\end{aligned} \tag{7}$$

where $\xi_k = \frac{4\pi}{3}N_A\sum_i r_i^k\bar{c}_i$.

The pressure-driven flow of the electrolyte through the charged soft channel induces a streaming field $\bar{E}_S$, which in turn develops a retarding EOF. Note that the electric field $\bar{E}_S$ due to the generation of SP is an unknown quantity. The fluid transport within the diffuse soft nanochannel governed by the applied pressure gradient and induced streaming field can be expressed based on the Darcy-Brinkman equation as

$$\rho(\bar{\mathbf{u}}.\bar{\nabla})\bar{\mathbf{u}} + \bar{\nabla}\bar{p} - \mu\bar{\nabla}^2\bar{\mathbf{u}} - \bar{\rho}_e\bar{\mathbf{E}}_S + \mu\ell^2\bar{\mathbf{u}} = 0 \tag{8}$$

$$\bar{\nabla}.\bar{\mathbf{u}} = 0 \tag{9}$$

where μ is the fluid viscosity, $\bar{p}$ is the pressure and $\bar{\mathbf{E}}_S$ is the induced streaming field. We introduce the dimensional quantities h (half channel height), $\bar{c_0}$ (bulk electrolyte concentration), $p_0(=\mu U_0/h)$, $\phi_0(=k_BT/ze)$ as the scale for length, ionic concentration, pressure, and EDL potential, respectively. Here $U_0=\frac{h^2}{2\mu}\left(-\frac{d\bar{p}}{dx}\right)$ is the reference velocity and pressure gradient $\left(-\frac{d\bar{p}}{dx}\right)$ is applied along the channel. The induced streaming field is scaled by ϕ_0/h. The bulk ionic strength of the electrolyte can be calculated as $I_0\left(=\frac{1}{2}\sum_i z_i^2\bar{c}_i^0\right)$. Using these scales, the governing equations can be written in nondimensional form as

$$-\nabla.[\{1-A(1-\epsilon_r)\}\nabla\phi]=\exp\left(-A\,\frac{\Delta W_i}{k_BT}\right)(kh)^2\rho_e+Q_{fix}\,g(y) \tag{10}$$

$$\nabla.\left[Pe_ic_i\mathbf{u}-\nabla c_i-z_ic_i\nabla\phi-c_i\nabla\ln\nu_i\right]=0 \tag{11}$$

$$Re(\mathbf{u}.\nabla)\mathbf{u}+\nabla p-\nabla^2\mathbf{u}-M\,\exp\left(-A\,\frac{\Delta W_i}{k_BT}\right)\rho_e\,\mathbf{E}_S+\beta^2g(y)\mathbf{u}=0 \tag{12}$$

$$\nabla.\mathbf{u}=0 \tag{13}$$

where $\beta=\ell_0h$ is the softness parameter of the PEL in terms of the reference screening length ℓ_0^{-1}. Here $k^{-1}=\sqrt{\epsilon_e\phi_0/2FI_0}$ is the EDL thickness and $Q_{fix}(=\rho_{fix}h^2/\epsilon_e\phi_0)$ is scaled fixed charge density of the PEL. The parameter $Pe_i=U_0h/D_i$ (i = 1,2,....N) is the Péclet number, which characterizes the ratio of ionic convection to diffusion. The ratio of dielectric permittivity of the PEL to the bulk electrolyte is denoted by $\epsilon_r=\epsilon_p/\epsilon_e$. The constant M appearing in Eq. (12) is $M=\frac{(kh)^2}{2}u_r$ where $u_r=U_{hs}/U_0$ is the ratio of electroosmotic velocity ($U_{hs}=\epsilon_e\phi_0^2/\mu h$) to the pressure-driven velocity scale (U_0). The distribution of the polymer segment inside the diffuse PEL can be written involving nondimensional variables as follows

$$g(y)=\frac{d_1}{\alpha_1\log\left(1+e^{2d_1/\alpha_1}\right)}\left[1-\tanh\left\{\frac{(1-y)-d_1}{\alpha_1}\right\}\right] \tag{14}$$

where the scaled PEL thickness and scaled decay length are defined as $d_1=d/h$ and $\alpha_1=\alpha/h$, respectively.

Along the upstream and downstream of the channel we impose the symmetry conditions for all flow variables ($\mathbf{u}$, c_i, ϕ). The rigid surface is considered to be non-slip and ion-impenetrable. The nondimensional form of the boundary condition along the channel wall ($y=1$) are as follows:

$$u=0,\quad v=0,\quad \epsilon_r\frac{\partial\phi}{\partial y}=-\sigma_s,\quad \left[\nabla c_i+z_ic_i\nabla\phi\right].\mathbf{n}=0 \tag{15}$$

where, σ_s is the scaled surface charge density, scaled by $\epsilon_e\phi_0/h$ and $\mathbf{n}$ is normal on the channel surface directing towards the fluid side. Along the centerline ($y=0$) symmetric boundary conditions are imposed:

$$\frac{\partial u}{\partial y}=0,\quad v=0,\quad \frac{\partial\phi}{\partial y}=0,\quad \frac{\partial c_i}{\partial y}=0 \tag{16}$$

It is interesting to note that the diffuse nature of the PEL grafted along the rigid walls of the channel allows us to avoid in considering the boundary condition along the PEL-to-electrolyte interface.

It may be noted that Eq. (12) involves $\mathbf{E}_S$, the electric field generated by the induced electrostatic potential due to the charged properties of the channel wall, PEL and the streaming potential. However, $\mathbf{E}_S$ is an unknown quantity a priori. The ionic current at a point in the flow domain is given by

$$I=u\sum_i z_ic_i-\sum_i\frac{1}{Pe_i}z_i\nabla c_i+E_S\sum_i\frac{1}{Pe_i}z_i^2c_i-\sum_i\frac{1}{Pe_i}z_ic_i\nabla\ln\nu_i \tag{17}$$

The axi-symmetric properties of the channel allows us to drop the diffusion current [47–50]. Thus, the net ionic current is given by

$$I_{net}=\underbrace{\int_0^1 u\left(\sum_i z_ic_i\right)dy}_{\text{streaming current}(I_s)}+\underbrace{E_S\int_0^1\left(\sum_i\frac{1}{Pe_i}z_i^2c_i\right)dy}_{\text{conduction current}(I_c)}-\underbrace{\int_0^1\left(\sum_i\frac{1}{Pe_i}z_ic_i\nabla\ln\nu_i\right)dy}_{\text{steric force induced current}(I_v)} \tag{18}$$

At the steady state, the net current I_{net} should be zero. Thus, from Eq. (18) we may obtain the streaming field along the axial direction as

$$E_S=\frac{\int_0^1\left(\sum_i\frac{1}{Pe_i}z_ic_i\nabla\ln\nu_i\right)dy-\int_0^1 u\left(\sum_i z_ic_i\right)dy}{\int_0^1\left(\sum_i\frac{1}{Pe_i}z_i^2c_i\right)dy} \tag{19}$$

The pressure-driven flow of electrolyte across the soft nanochannel experiences a resistance which arises due to the opposing EOF induced by the streaming field. As a result the net flow rate reduces compared to the pressure-driven Poiseuille flow due to the coupling of the electrostatics and hydrodynamic forces. This can be viewed as an increase in effective viscosity and such phenomenon termed as the

electroviscous effect (EVE) [4, 5, 9, 47]. The enhanced effective viscosity can be measured by the ratio of net flow rate considering only a pressure gradient-driven flow (with no electrokinetic effects) to the net flow rate as that due to pressure-driven electrokinetic flow. Thus, the enhanced viscosity (μ_{eff}) scaled by the original viscosity of the aqueous medium, can be expressed as [51]

$$\frac{\mu_{eff}}{\mu} = \frac{\int_0^1 u_p \, dy}{\int_0^1 u \, dy} \tag{20}$$

where u_p is the dimensionless pure pressure-driven velocity field (without considering the electrokinetic effects).

The efficiency of electrochemomechanical energy conversion is one of the most important key factor for energy conversion systems, which can directly be measured by considering the ratio of input power to the output power, as follows [3, 18]

$$\Theta = \frac{P_{out}}{P_{in}} \tag{21}$$

The input power (P_{in}) can be expressed as $P_{in} = \left| -\frac{dp}{dx} Q_p \right|$. Here Q_p is the volume flow rate due to purely pressure-driven flow (i.e., $\sigma = N = 0$) through the soft channel $Q_p = 2\int_0^1 u_p \, dy$. The electrical energy associated with the generation of the streaming potential, i.e., P_{out} is given by $P_{out} = \frac{I_s}{2}\frac{E_S}{2}$, where I_s is the streaming current given by $I_s = 2\int_0^1 u\left(\sum_i z_i c_i\right) dy$.

Numerical method

The governing Eqs. (10–12) are nonlinear coupled set of partial differential equations, which are solved using the numerical scheme based on finite volume method. A control volume approach over a staggered grid system is adopted to discretize the governing equations. We have employed the QUICK (Quadratic Upstream Interpolation for Convective Kinematics) scheme [52] to discretize the convection and electromigration terms (i.e., hyperbolic terms) and the second order central difference scheme is used for the diffusion term (i.e., elliptic term). We first solve the discretized equation for electrostatic potential iteratively with the guess value of ionic concentrations. With known value of potential field and a guess value of velocity field, we have solved iteratively the discretized equations of concentration of ionic species. Solutions of discretized equations for electrostatic potential and concentration equations are quite straightforward; however, the solution of flow equations is significantly difficult because it is coupled to the streaming field, governed by Eq. (19). To overcome this complexity we further adopt an iterative scheme to obtain the streaming field and flow field. We adopt the pressure correction based iterative algorithm SIMPLE (Semi-Implicit Method for Pressure-Linked Equations) [53] to solve the velocity field. At each iteration based on the velocity, we determine the streaming field by Eq. (19). Iteration process is continued until the difference in E_S in two successive iterations is smaller than 10^{-6}. In order to validate the numerical results, we have compared our computed results for streaming potential with the existing results. A detailed discussion on the code validation is provided in the Appendix.

Results and discussion

The diffusivity and size of constituent electrolyte ions are summarized in Table 1. The concentration of the background electrolyte is varied from low (1 mM) to high (100 mM) [54], so that the Debye-Hückel parameter κh ranges from 2.6 to 26 for the channel of height $2h = 50$ nm. We consider the variation of the concentration of PEL immobile ions from 0 to 30 mM, so that the magnitude of ρ_{fix} can range from 0 to 2.89×10^6 C/m^3 [30, 55]. The dielectric permittivity of the PEL ranges from $0.5\epsilon_e$ to ϵ_e [30], where ϵ_e is the dielectric permittivity of the background electrolyte, which is $80 \times 8.854 \times 10^{-12}$ F/m. The softness parameter β is considered to vary between 1 to 10, which correspond to the variation of PEL screening length between 2.5 nm to 25 nm. Such a range of PEL screening length for soft nanofluidic channels is considered by Duval et al. [22]. Following the experimental studies [56–58] for silica nanochannels, the surface charge density (σ) for the present study is varied up to -70 mC m^{-2}.

Impact of ion partitioning

The Donnan potential created by the PEL charge density affects the development of the EDL and its impact on the EDL is strong for lower ionic concentration for which the Debye layer extends beyond the PEL. The effective charge density of the PEL depends on the counterion condensation and electroosmsois of the mobile ions. The impact of ion partitioning

Table 1 The hydrated radius and diffusivity of electrolyte ions are shown

Ions	K^+	Na^+	Li^+	Cl^-	Ba^{2+}	Al^{3+}
r_i (Å)	3.31	3.58	3.82	3.32	4.04	4.75
$D_i \times 10^{-9}$ (m^2/s)	1.96	1.33	1.03	2.03	0.8471	0.559

and ion steric interactions on the average charge density in the PEL (Q_{eff}) and the surface potential of the channel wall is presented in Fig. 2a, b for $\kappa h = 2.5$ ($C_0 = 1$ mM) by considering the variation of the PEL-to-electrolyte dielectric permittivity ratio (ϵ_r) for salts of different counterion size (e.g., KCl, NaCl, and LiCl). The average charge density Q_{eff} in the PEL is determined as

$$Q_{eff} = \frac{1}{\bar{d}/h} \int_{1-\bar{d}/h}^{1} \left[(kh)^2 \left(\sum_i z_i f_i c_i \right) + Q_{fix} g(y) \right] dy$$

For a soft channel with uncharged wall coated with negatively charged PEL with $N = 30$ and $z = -1$, the penetration of counterions reduces the effective PEL charge. For such a case the average charge density Q_{eff} in the PEL is negative, dominated by the PEL immobile charges. When the surface is negatively charged it draws positive counterions in the vicinity of the charged surface, creating a strong shielding of the PEL immobile negative charge. At a large $\sigma(= -50$ mC m^{-2}) the density of the mobile counterions (positive ions) becomes so large that the net charge in the PEL region becomes positive. Thus, Q_{eff} becomes opposite sign to that of the Q_{fix} due to the dominance of the all induced mobile counterions in the PEL (Fig. 2a). As ϵ_r is increased (PEL permittivity becomes higher) the ion partitioning effect diminishes, which causes a larger accumulation of counterions in the PEL. Higher concentration of counterions leads to higher counterion condensation, leading to a lower effective charge density of the PEL.

Larger accumulation of counterions also creates a reduction in the surface potential (Fig. 2b) by enhancing the shielding effect. The saturation of counterions due to the ion steric interactions attenuates the shielding effect. For this, both Q_{eff} and ϕ_w becomes larger when steric effect is considered (Fig. 2a, b). This steric interaction is stronger for a larger size counterion, and thus, the shielding effect

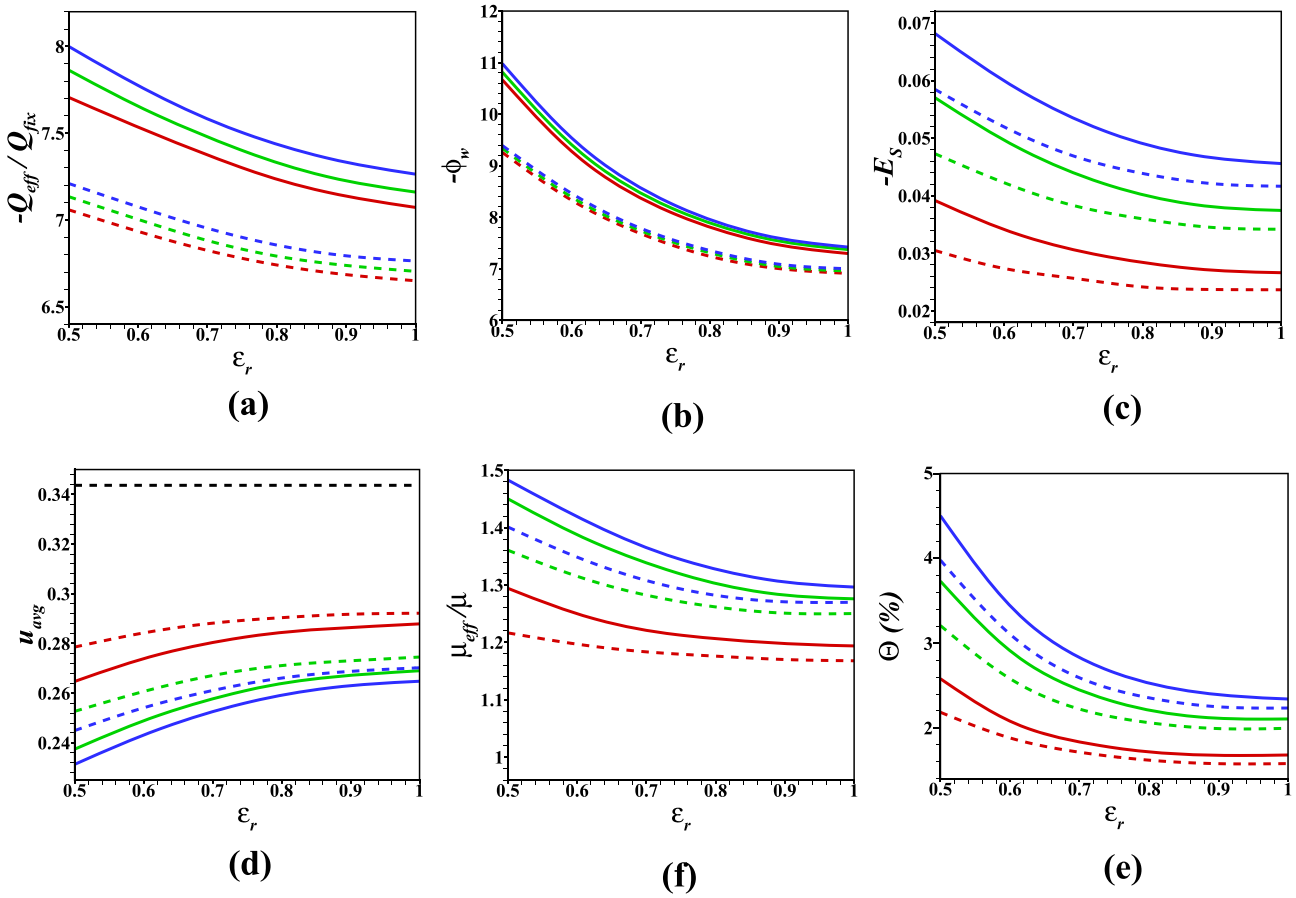

Fig. 2 Dependence of the scaled **a** Q_{eff}/Q_{fix}, **b** surface potential (ϕ_w), **c** streaming potential (E_S), **d** average velocity (u_{avg}), **e** enhanced viscosity (μ_{eff}/μ), (f) efficiency of the electrochemomechanical energy conversion (Θ) on ϵ_r when $C_0 = 1$ mM ($\kappa h = 2.5$), $\sigma = -50$ mC m^{-2}, $N = 30$ mM and $z = -1$, $\beta = 1$, $\alpha/h = 0.1$, $h = 25$ nm. Different electrolytes are taken as, KCl (red); NaCl (green); LiCl (blue). Dashed lines represent the corresponding case for $\chi = 0$ (no steric effect). The horizontal black color dashed line in Fig. 2d corresponds the average flow rate for the pressure-driven flow without considering the impact of induced SP

reduces leading to larger Q_{eff} and ϕ_w. It may be noted that higher counterion size posseses a lower diffusivity, which also attenuates the PEL counterion condensation leading to a higher Q_{eff}. We find that the impact of the steric interactions magnifies for the lower range of the PEL-to-electrolyte dielectric permittivity ratio for which the ion partitioning effect is stronger.

For the channel with negatively charged walls coated with negatively charged PELs, the counterions (cations), which are driven downstream by the imposed pressure bias, generate a negative streaming field. The streaming electric field E_S arises due to the streaming current in the channel, which creates a reverse conduction current. Figure 2c shows that the streaming field attenuates as the dielectric permeability of the PEL enhances. Increase in the PEL-to-electrolyte dielectric permittivity ratio (ϵ_r) diminishes the ion partitioning effect, which causes more counterions to accumulate within the PEL. Higher accumulation of mobile counterions in PEL enhances the counterion condensation by the shielding effect to cause the reduction of the PEL effective charge density. Consideration of ion steric interactions in the ion transport equation creates an enhanced E_S and the impact is higher for lower range of ϵ_r for which the ion partitioning is stronger. As discussed before, the depletion of counterions in EDL due to ions steric interactions and ion partitioning attenuates shielding effect of the surface charge leading to higher streaming current and hence, higher E_S. We find that the consideration of the steric interactions creates a 17.81% increment in E_S for LiCl when $\epsilon_r = 0.5$.

The streaming potential retards the fluid flow through the channel. For this, as seen in Fig. 2d, the pattern of dependence of the cross-sectional averaged velocity u_{avg} on the electrokinetic parameters is opposite to the pattern of dependence of streaming potential. It enhances as the ion partitioning effect diminishes, i.e., ϵ_r is increased as well as when the steric effect is not taken into account (Fig. 2d). The velocity depends on the imposed pressure gradient and induced streaming field. A reduced streaming field reduces the opposing EOF leading to an enhanced u_{avg}. The ion steric interaction creates a reduction in u_{avg} by enhancing the adverse EOF and this impact becomes stronger for salts of larger counterion size. The scaled effective viscosity μ_{eff}/μ is presented in Fig. 2e as a function of ϵ_r for different types of salts with or without ion steric effects. The effective viscosity is higher than 1 as the streaming field resists the pressure-driven flow, which in turn attenuates the net flow. The variation of the effective viscosity with ϵ_r follows the similar pattern as that of the streaming field. At a fixed ϵ_r, μ_{eff}/μ is enhanced due to the steric interactions as the streaming field becomes stronger.

The electrochemomechanical energy conversion efficiency is defined as the ratio of the amount of extractable electrical energy due to the induced electrical field to the amount of power required to generate the flow. The conversion of the mechanical energy to the electrical energy leads to the generation of the streaming current and the streaming electric field. The efficiency of such process is measured through the factor Θ, as defined in Eq. (21). Figure 2f shows that the energy conversion efficiency is high for lower values of the PEL-to-electrolyte dielectric permittivity ratio for which the concentration of the mobile counterions in the PEL is low due to ion partitioning. As ϵ_r is increased the streaming field reduces as well as the streaming current reduces. The ion steric interactions augment the efficiency factor Θ due to the increment of E_S. We find that for $\epsilon_r = 0.5$ an increment of 12.63% in Θ occurs when the steric interaction is considered for the LiCl salt.

Effect of surface charge density

The impact of surface charge density on the streaming potential, average velocity and EVE is illustrated in Fig. 3a–c. We have presented results for a soft nanochannel with uncharged as well as charged PEL. We have considered both the cases when the PEL bears similar or opposite charges to that of the channel walls. Results are presented here for low concentration of the background electrolytic so that the surface charge density plays an important role on the electrohydrodynamics. At a thicker Debye length (lower c_0) for which Debye layers overlaps, the ion conduction dominates the ion convection. We find that for the case of uncharged PEL ($N = 0$), the magnitude of the negative streaming field increases by a small margin as the surface charge density is increased as the number density of counterions in the channel increases. For a soft nanochannel with similarly charged PEL and channel walls (both are negative), the counterions (positive ions) are driven along the downstream by the applied pressure gradient, leading to a negative streaming field. For a weakly charged surface the streaming field is large and is governed by the counterions drawn by the PEL negative charge. This negative streaming field attenuates as the surface charge density is increased. This is justified as the rise in negative surface charge enhances the accumulation of counterions in the EDL, which manifests the counterion condensation of the PEL, leading to a reduction in PEL effective charge density. For a higher $-\sigma$, the streaming field asymptotically approaches to that of the soft nanochannel with uncharged PEL and negatively charged walls as the mobile counterions in the wall induced EDL shields the PEL immobile ions of opposite polarity.

When the PEL is positively charged (opposite to that of the channel walls) and the surface is weakly charged, the ion transport is dominated by the charge properties of the PEL and a positive streaming field develops due to migration of anions (counterions with respect to the PEL charge) under the applied pressure-driven flow. This positive streaming

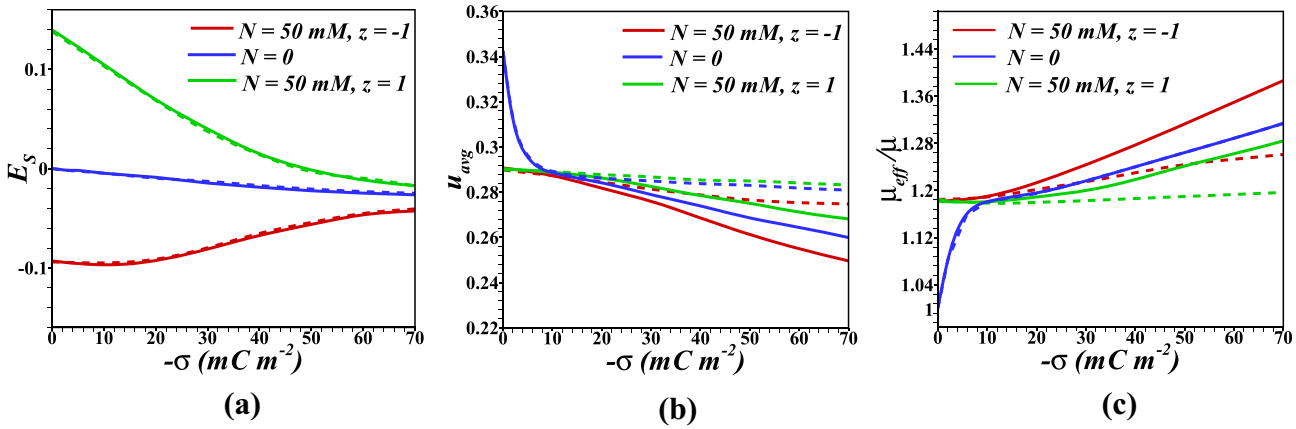

Fig. 3 Dependence of the **a** streaming potential (E_S), **b** average velocity (u_{avg}), **c** enhanced viscosity (μ_{eff}/μ) on σ when $c_0 = 1$ mM, $N = 50$ mM and $z(= -1, 1)$, $\epsilon_r = 0.5$, $\beta = 1$, $\alpha/h = 0.1$. Dashed lines represent the corresponding case for $\chi = 0$ (no steric effect)

field gradually diminishes as $-\sigma$ is increased and approaches to that of the channel with uncharged PEL. It is evident from Fig. 3a that the ion steric interaction reduces the streaming field by a small margin by creating a counterion saturation.

Figure 3b shows that when the channel walls are weakly charged, the average velocity is significantly lower (and hence the effective viscosity is higher, Fig. 3c) than that of the soft nanochannel with uncharged PEL ($N = 0$). For a higher range of surface charge density both u_{avg} and μ_{eff} of the soft channel become close to the case of the uncharged PEL. A rise in surface charge density enhances the migration of counterions towards the downstream of the channel, resulting in a reduced (enhanced) u_{avg} (effective viscosity), and its impact is more pronounced when the PEL and channel walls are similarly charged. However, for a channel with oppositely charged walls and PELs, the EDL mediated counterions screen the PEL charges leading to a higher u_{avg} (lower μ_{eff}) compared to that of the channel with similarly charged PEL and walls.

We have seen (not presented here for the sake of brevity) that the efficiency factor for the uncharged PEL when varied with the wall charge density (σ) attains a local maximum at a higher σ. Further increase in σ leads to a reduction in Θ. A similar finding has already been reported in literature by Buren et al. [59] for a bare nanochannel with charged walls. The efficiency factor could be enhanced when PEL charge has the same polarity ($z = -1$) as that of the wall charge. We found that at $\sigma = -50$ mC m^{-2}, Θ is increased by 20.81% when PEL charge density is increased from $N = 10$mM to 50mM and $z = -1$. Further increase of $-\sigma$ attenuates Θ.

Effect of the bulk ionic concentration

In Fig. 4a–c we have presented the impact of ionic concentration on the generation of SP, effective viscosity and the average velocity. The results are presented here for surface charge density $\sigma = -30$ mC m^{-2} and highly charged PEL with positive as well as negative polarity ($z = 1, -1$). In all the cases the magnitude of E_S is higher for lower range of the bulk ionic concentration, i.e., lower values of κh, as the conduction current augments when the bulk ionic concentration is increased. Thus, the effective viscosity is higher compared to fluid viscosity, i.e., $\mu_{eff}/\mu > 1$. Based on the Debye-Hückel approximation Chanda et al. [18] have demonstrated that for a soft nanochannel with uncharged walls, $E_S \sim 1/(\kappa h)^2$ for a low to moderate range of EDL thickness and further increase of EDL thickness creates E_S to approach a saturation. A similar trend in variation of E_S with κh is observed when both the PEL and channel walls are similarly charged ($z = -1$). In this case the magnitude of streaming potential reduces with the rise in concentration of electrolyte. The positively (negatively) charged PEL induces a positive (negative) streaming potential. At a low electrolyte concentration, the counterion condensation of the PEL is low and hence, the impact of PEL charge dominates, which results in the positive streaming potential. With the rise of c_0 the effective charge density of PEL reduces due to the stronger screening effect, which attenuates the SP. At a larger value of c_0, the E_S of the soft channel approaches to the value corresponding to the case of $N = 0$ (uncharged PEL).

With the increase of c_0 the average velocity (Fig. 4b) increases and approaches the corresponding pressure-driven Poiseuille flow and hence, the effective viscosity approaches to that of the viscosity of the electrolyte. We find from Fig. 4c that the effective viscosity is increased when ion steric effect is considered and the impact is strong at a larger σ. This is expected as the ion steric interactions attenuate accumulation of counterions, leading to an enhancement of PEL effective charge density, which in turn inhibits the average flow, and, hence, enhance the effective viscosity.

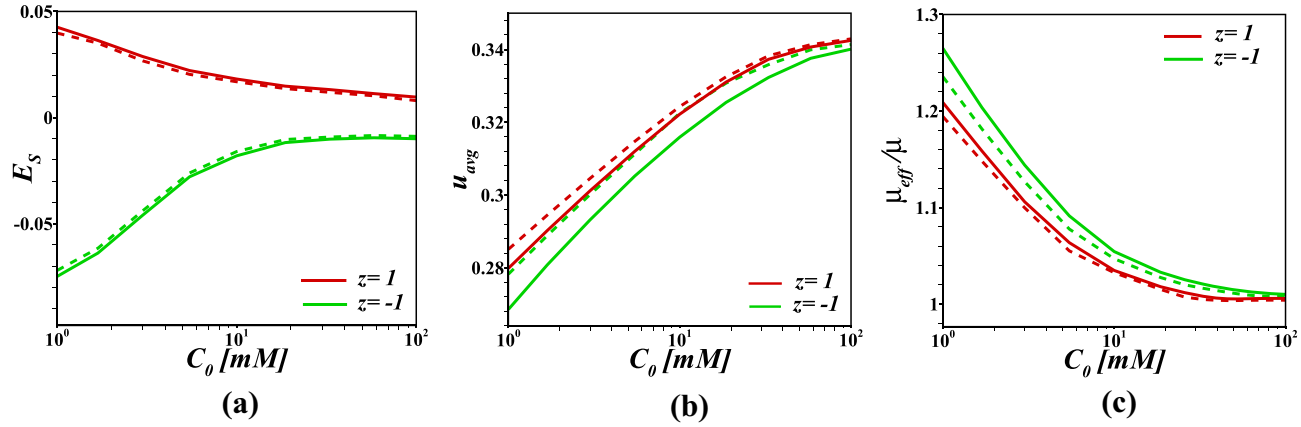

Fig. 4 Dependence of the **a** streaming potential (E_S), **b** average velocity (u_{avg}), **c** enhanced viscosity (μ_{eff}/μ) on c_0 when $\sigma = -30$ mC m^{-2}, $N = 50$ mM and $z(= -1, 1)$, $\epsilon_r = 0.5$, $\beta = 1$, $\alpha/h = 0.1$. Dashed lines represent the corresponding case for $\chi = 0$ (no steric effect)

We observed that the energy conversion efficiency factor Θ (results are not presented for sake of brevity) reduces rapidly as the bulk ionic concentration is increased and approaches to zero for sufficiently concentrated aqueous medium. This is expected as the electric power attenuates with the increase of c_0.

Impact of PEL thickness

The impact of scaled PEL thickness (d/h) and softness parameter (β) on the generation of SP, associated EVE and energy conversion is illustrated in Fig. 5a–c for a lower bulk ionic concentration for which the impact is high. The immobile ions of the PEL are considered to have the same polarity as that of the surface charge so as to have a higher conversion efficiency factor. We have also included the results of the corresponding rigid nanochannel, i.e., $d = 0$. When the PEL is highly permeable (low β) the Donnan potential created by the PEL fixed charge density creates a strong streaming current and hence, enhanced SP. However, E_S reduces when the PEL becomes less permeable as the conduction current enhances as well as streaming current attenuates due to lower ion convection. The SP is an increasing function of the PEL thickness for larger range of PEL pore size (lower β) and it monotonically reduces as the PEL thickness is increased for the dense PEL (larger β). An enhanced SP is observed considering the impact of ion size and a maximum deviation of 7.81% in SP obtained for approach-1 (results considering the impact of ion size) and approach-2 (results neglecting the impact of ion size) is possible for $c_0 = 1$ mM and thick PEL.

Figure 5b depicts the EVE when the thickness of the charged PEL (d) is varied at different permeability. Increase

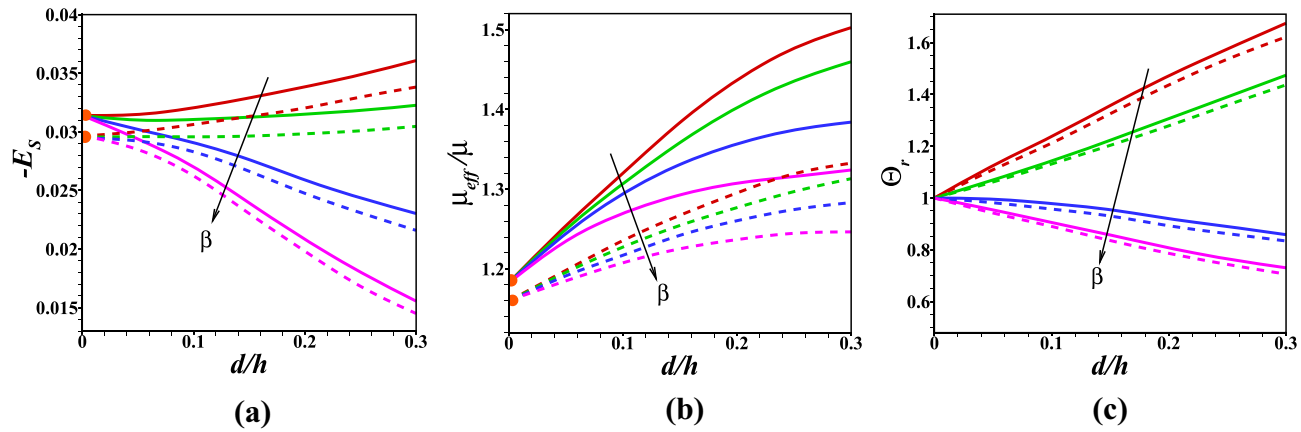

Fig. 5 Dependence of the **a** streaming potential (E_S), **b** enhanced viscosity (μ_{eff}/μ), **c** efficiency of the electrochemomechanical energy conversion rate (Θ_r) on PEL thickness ($d_1 = d/h$) for different $\beta(= 1, 2, 5, 10)$ when $C_0 = 1$ mM, $\epsilon_r = 0.5$, $\sigma = -50$ mC m^{-2}, $N = 30$ mM and $z = -1$, $\alpha/h = 0.1$. Here the background electrolyte is taken as KCl. Dashed lines represent the corresponding case for $\chi = 0$ (no steric effect). Orange symbols represent the corresponding result for rigid channel

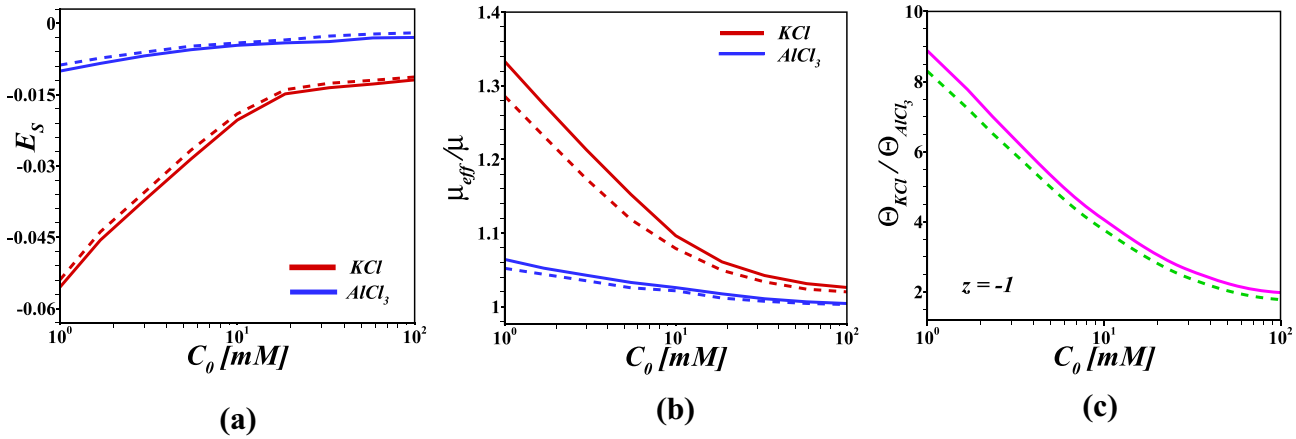

Fig. 6 Dependence of the **a** streaming potential (E_S), **b** enhanced viscosity (μ_{eff}/μ), **c** ratio of efficiency of the electrochemomechanical energy conversion ($\Theta_{KCl}/\Theta_{AlCl_3}$) on C_0 when $\sigma = -50$ mC m^{-2}, $N = 30$ mM and $z = -1$, $\epsilon_r = 0.5$, $\beta = 1$, $\alpha/h = 0.1$. Dashed lines represent the corresponding case for $\chi = 0$ (no steric effect)

in d enhances the density of the effective immobile charge of the PEL, which creates an enhancement in opposing EOF and thereby a reduction in the net flow rate. For this the effective viscosity $\mu_{eff} > \mu$ and this effect is stronger for highly permeable PEL as the streaming field becomes higher. Compared to the pressure-driven flow, a maximum percentage difference of 12.11% and 13.28% occurs for u_{avg} and μ_{eff}/μ, respectively. Figure 5c shows that the energy conversion efficiency factor Θ increases rapidly with the PEL thickness for smaller value in softness parameter (β). However, a reduction in Θ with PEL thickness occurs for moderate to higher value in β for which the streaming field reduces gradually. For a soft nanochannel with highly (weakly) permeable PEL, the efficiency factor Θ increases (reduces) up to 1.7 times (0.8 times) of the corresponding rigid nanochannel. We further observed a maximum percentage difference of 4.08% occurs when ion steric effect is incorporated in the transport equation.

Valence asymmetric salts

The combined effect of surface charge density and the fixed charge density of the PEL on the streaming potential and the associated EVE for different types of salts are shown when PEL and walls are similarly charged (Fig. 6) and oppositely charged (Fig. 7). As the bulk electrolyte concentration is decreased, the convection of mobile ions within the thicker Debye layer enhances, and thus, the net flow rate (u_{avg}) reduces, which in turn produces a higher EVE and energy efficiency. This impact is significant when a monovalent salt

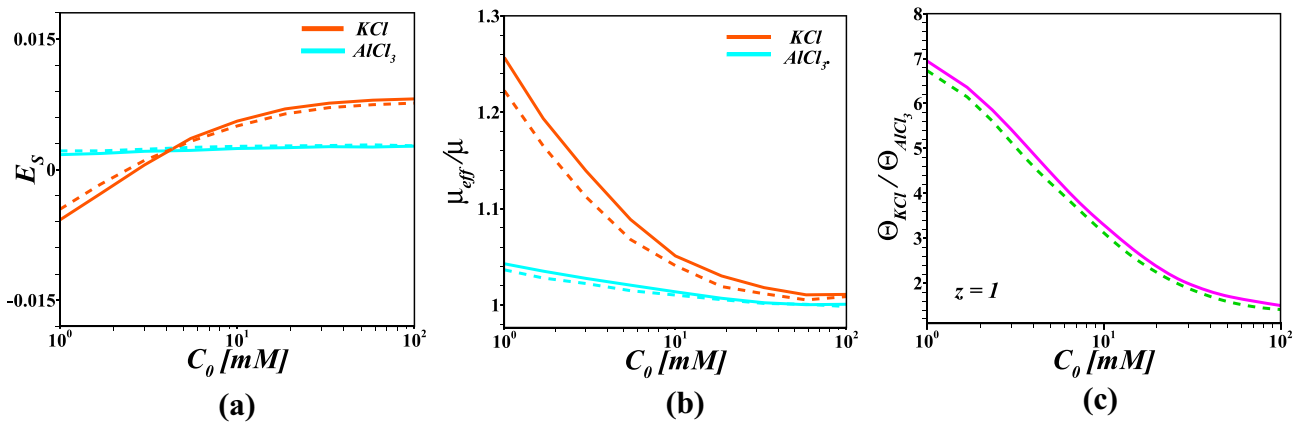

Fig. 7 Similar set of results as shown in Fig. 6 for the case when the channel walls and PELs are similarly charged ($\sigma = -50$ mC m^{-2}, $N = 30$ mM and $z = 1$). Dashed lines represent the corresponding case for $\chi = 0$ (no steric effect). Other model parameters are same as considered in Fig. 6

is considered as it produces a higher streaming current as a result of higher rate of convection of ions, whereas for multivalent counterions, shielding effect increases as the higher valent ion has higher charge and stronger Columbic repulsion force among themselves. Thus, the effective surface potential reduces, which in turn produces a lower SP compared to the monovalent salt. As the bulk electrolyte concentration is increased, the EDL contracts, and thus, the effective charge density of the PEL and the impact of wall surface charge reduces. The net flow rate (u_{avg}) increases as a result of lower electroosmotic transport of mobile ions within the thin Debye layer. The associated EVE and the energy efficiency become lower as a result of the reduced streaming field. For a monovalent salt, the surface charge density plays a dominant role when the PEL and the walls are oppositely charged ($z = 1$) and the bulk electrolyte concentration is low. Thus, the streaming field is negative. The impact of surface charge density reduces as the bulk electrolyte concentration is increased and the streaming field switches its direction from negative to positive for a monovalent salt (Fig. 7a). However, for higher valent salt, due to increased shielding effect of surface charge, the induced SP is very low and consequently, EVE is also smaller. Figures 6c and 7c show that the energy conversion efficiency becomes significantly higher for the KCl solution compared to that of $AlCl_3$ aqueous solution. This is justified as the induced streaming current is higher for the monovalent KCl salt. The energy conversion efficiency attenuates as c_0 is increased. We have also analyzed the SP by considering the background aqueous medium as a mixture of monovalent and multivalent electrolytes with various proportion ratios. The corresponding results are presented in Supplementary material. We found that the impact of the proportion ratio of the constituent salts in the mixed electrolyte is found to have less impact on the generation of streaming potential and associated EVE.

Conclusions

The streaming electric field and electroviscous effects induced by a pressure-driven flow of electrolytes in a soft channel are studied numerically. A diffuse polyelectrolyte layer (PEL) having a fixed volume charge density is considered to be grafted on the inner sides of the microchannel charged walls. The dielectric permittivity of the PEL is lower than the aqueous medium, which creates a Born energy difference of the ions. The Nernst-Planck-Poisson model for electrokinetic transport is modified to incorporate the ion steric repulsion due to finite ion size consideration and the ion partitioning effect arises due to the Born energy difference. Due to this modification the present model is applicable for higher range of charge density as well as larger ionic concentration in the EDL. We have compared the present model with several existing results and established an excellent agreement. The streaming field, electroviscous effect and energy conversion efficiency of the soft channel are analyzed by varying the electrokinetic parameters. We have considered the electrolyte as the mixture of salts of different ion size and valence.

The present study shows that for the highly permeable PEL possessing charge of same polarity as that of the wall produces a higher streaming field and energy conversion efficiency. This impact of the PEL becomes significant for the lower range of the bulk ionic concentration. The streaming field augments when the dielectric permittivity of the PEL becomes lower than the electrolyte medium, i.e., the ion partitioning effect becomes significant. The streaming field increases as the counterion ion size is increased. However, it decreases for an electrolyte with multivalent counterion. We have shown (Supplementary material) that an electrolyte solution consists of the mixture of NaCl with a salt of monovalent counterion of higher ion size or multivalent counterion can produce a significant influence in the energy conversion efficiency.

Appendix

Comparison of computed results with the existing studies

In Fig. 8 we have presented a comparison of our computed results for the electrostatic potential on a planner rigid surface bearing the surface charge density $\sigma = 10, 20, 50\,\text{mC m}^{-2}$ with the theoretical results obtained by Ohshima [60] and numerically computed results by López-García et al. [36]. For the sake of comparison with those existing results we have adopted the CS model for ion steric effect in which the size of the hydrated ions are considered to be the same. We find a close agreement of our computed results with these existing results.

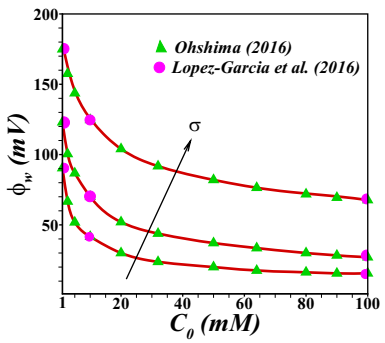

Fig. 8 Dependence of the surface potential (ϕ_w) on a planar charged surface in contact with an electrolyte solution. The results are presented here as a function of C_0 when $\sigma = 10, 20, 50$ mC m^{-2} and $r_i = 0.4$ nm. We have also included the results by Ohshima [60] and López-García et al. [36], represented by the symbols

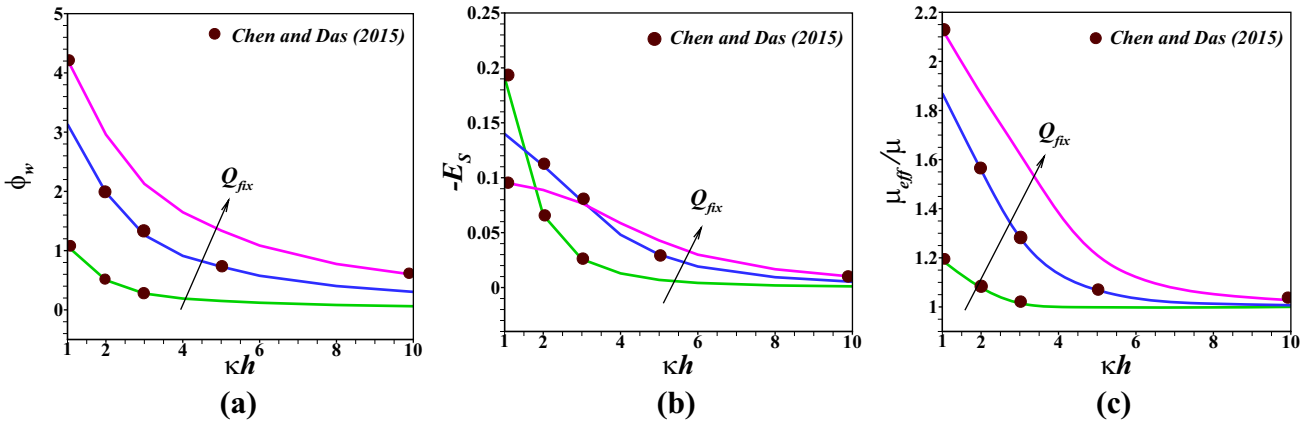

Fig. 9 Dependence of the dimensionless **a** surface potential (ϕ_w), **b** streaming potential (E_S), **c** effective viscosity (μ_{eff}/μ) for soft channel as a function of κh when $\sigma = 0$, $\epsilon_r = 1$, $\beta = 1$, $d/h = 0.1$. The results are presented here for different values of $Q_{fix} = 10, 50, 100$. The arrow represents the increasing direction of Q_{fix}. The symbols refers the results by Chen and Das [51]

In Fig. 9 we have presented comparison of wall potential, streaming field and effective viscosity for soft nanochannel. The results are presented for the similar sets of parameters considered by Chen and Das [51] for soft nanochannel with step-like PEL ($\alpha = 0$) and uncharged channel walls ($\sigma = 0$). We have established a close agreement of our computed results with those already derived by Chen and Das [51]. It may be noted that in Fig. 9, the results are based on the Boltzmann distribution of ions which neglects the effect of ion steric interactions (i.e., $\chi = 0$) and ion partitioning (i.e., $\epsilon_r = 1$).

Supplementary Information The online version contains supplementary material available at https://doi.org/10.1007/s00396-022-05007-8.

Funding S.B. acknowledge the financial support received from the Science and Engineering Research Board, Govt. of India, under grant no. MTR/2021/000020. P.P.G acknowledge the financial support received from the National Institute of Technology Durgapur through the project grant under "Research Initiation Grant".

Declarations

Conflict of interest The authors declare no competing interests.

References

1. van der Heyden FHJ, Stein D, Dekker C (2005) Streaming currents in a single nanofluidic channel. Phys Rev Lett 95(11):116104
2. Siria A, Poncharal P, Biance A-L, Fulcrand R, Blase X, Purcell ST, Bocquet L (2013) Giant osmotic energy conversion measured in a single transmembrane boron nitride nanotube. Nature 494(7438):455–458
3. Daiguji H, Yang P, Szeri AJ, Majumdar A (2004) Electrochemomechanical energy conversion in nanofluidic channels. Nano Lett 4(12):2315–2321
4. Das T, Das S, Chakraborty S (2009) Influences of streaming potential on cross stream migration of flexible polymer molecules in nanochannel flows. J Chem Phys 130(24):244904
5. Das S, Guha A, Mitra SK (2013) Exploring new scaling regimes for streaming potential and electroviscous effects in a nanocapillary with overlapping electric double layers. Anal Chim Acta 804:159–166
6. Ho C-M, Tai Y-C (1998) Micro-electro-mechanical-systems (MEMS) and fluid flows. Annu Rev Fluid Mech 30(1):579–612
7. Li D (2001) Electro-viscous effects on pressure-driven liquid flow in microchannels. Colloids Surf, A 195(1–3):35–57
8. Davidson MR, Harvie DJE (2007) Electroviscous effects in low reynolds number liquid flow through a slit-like microfluidic contraction. Chem Eng Sci 62(16):4229–4240
9. Bharti RP, Harvie DJE, Davidson MR (2008) Steady flow of ionic liquid through a cylindrical microfluidic contraction-expansion pipe: electroviscous effects and pressure drop. Chem Eng Sci 63(14):3593–3604
10. Vázquez-Quesada A, Ellero M, Español P (2009) Consistent scaling of thermal fluctuations in smoothed dissipative particle dynamics. J Chem Phys 130(3):034901
11. Yang J, Lu F, Kostiuk LW, Kwok DY (2003) Electrokinetic microchannel battery by means of electrokinetic and microfluidic phenomena. J Micromech Microeng 13(6):963
12. Donath E, Voigt A (1986) Streaming current and streaming potential on structured surfaces. J Colloid Interface Sci 109(1):122–139
13. Ohshima H, Kondo T (1990) Electrokinetic flow between two parallel plates with surface charge layers: electro-osmosis and streaming potential. J Colloid Interface Sci 135(2):443–448
14. Starov VM, Solomentsev YE (1993) Influence of gel layers on electrokinetic phenomena: 1. streaming potential. J Colloid Interface Sci 158(1):159–165
15. Keh HJ, Liu YC (1995) Electrokinetic flow in a circular capillary with a surface charge layer. J Colloid Interface Sci 172(1):222–229
16. Keh HJ, Ding JM (2003) Electrokinetic flow in a capillary with a charge-regulating surface polymer layer. J Colloid Interface Sci 263(2):645–660
17. Nguyen T, Xie Y, de Vreede LJ, van den Berg A, Eijkel JC (2013) Highly enhanced energy conversion from the streaming current by polymer addition. Lab Chip 13(16):3210–3216
18. Chanda S, Sinha S, Das S (2014) Streaming potential and electroviscous effects in soft nanochannels: towards designing more efficient nanofluidic electrochemomechanical energy converters. Soft Matter 10(38):7558–7568
19. Chen G, Patwary J, Sachar HS, Das S (2018) Electrokinetics in nanochannels grafted with poly-zwitterionic brushes. Microfluid Nanofluid 22(10):1–19

20. Chen G, Sachar HS, Das S (2018) Efficient electrochemomechanical energy conversion in nanochannels grafted with end-charged polyelectrolyte brushes at medium and high salt concentration. Soft Matter 14(25):5246–5255
21. Patwary J, Chen G, Das S (2016) Efficient electrochemomechanical energy conversion in nanochannels grafted with polyelectrolyte layers with ph-dependent charge density. Microfluid Nanofluid 20(2):1–14
22. Duval JFL, Zimmermann R, Cordeiro AL, Rein N, Werner C (2009) Electrokinetics of diffuse soft interfaces. iv. analysis of streaming current measurements at thermoresponsive thin films. Langmuir 25(18):10691–10703
23. Duval JF, Küttner D, Werner C, Zimmermann R (2011) Electrohydrodynamics of soft polyelectrolyte multilayers: point of zero-streaming current. Langmuir 27(17):10739–10752
24. Andrews J, Das S (2015) Effect of finite ion sizes in electric double layer mediated interaction force between two soft charged plates. RSC Adv 5(58):46873–46880
25. Young M, Jayaram B, Beveridge D (1998) Local dielectric environment of B-DNA in solution: Results from a 14 ns molecular dynamics trajectory. J Phys Chem B 102(39):7666–7669
26. Ganjizade A, Ashrafizadeh SN, Sadeghi A (2017) Effect of ion partitioning on the electrostatics of soft particles with a volumetrically charged core. Electrochem Commun 84:19–23
27. Mahapatra P, Gopmandal PP, Duval JF (2021) Effects of dielectric gradients-mediated ions partitioning on the electrophoresis of composite soft particles: An analytical theory. Electrophoresis 42(1–2):153–162
28. Heyde M, Peters C, Anderson J (1975) Factors influencing reverse osmosis rejection of inorganic solutes from aqueous solution. J Colloid Interface Sci 50(3):467–487
29. Born M (1920) Volumen und hydratationswärme der ionen. Zeitschrift für Physik 1(1):45–48
30. Poddar A, Maity D, Bandopadhyay A, Chakraborty S (2016) Electrokinetics in polyelectrolyte grafted nanofluidic channels modulated by the ion partitioning effect. Soft Matter 12(27):5968–5978
31. Bikerman J (1942) Xxxix. structure and capacity of electrical double layer. The London, Edinburgh, and Dublin Philosophical Magazine and Journal of Science 33(220):384–397
32. Koranlou A, Ashrafizadeh SN, Sadeghi A (2019) Enhanced electrokinetic energy harvesting from soft nanochannels by the inclusion of ionic size. J Phys D: Appl Phys 52(15):155502
33. Xing J, Jian Y (2018) Steric effects on electroosmotic flow in soft nanochannels. Meccanica 53(1):135–144
34. Carnahan NF, Starling KE (1969) Equation of state for nonattracting rigid spheres. J Chem Phys 51(2):635–636
35. López-García JJ, Horno J, Grosse C (2015) Influence of steric interactions on the dielectric and electrokinetic properties in colloidal suspensions. J Colloid Interface Sci 458:273–283
36. López-García JJ, Horno J, Grosse C (2016) Ion size effects on the dielectric and electrokinetic properties in aqueous colloidal suspensions. Curr Opin Colloid Interface Sci 24:23–31
37. Biesheuvel PM, Van Soestbergen M (2007) Counterion volume effects in mixed electrical double layers. J Colloid Interface Sci 316(2):490–499
38. López-García JJ, Horno J, Grosse C (2014) Influence of the finite size and effective permittivity of ions on the equilibrium double layer around colloidal particles in aqueous electrolyte solution. J Colloid Interface Sci 428:308–315
39. López-García J, Horno J, Grosse C (2018) Diffuse double-layer structure in mixed electrolytes considering ions as dielectric spheres. The European Physical Journal E 41(9):1–9
40. Pandey D, Bhattacharyya S (2021) Impact of finite ion size, born energy difference and dielectric decrement on the electroosmosis of multivalent ionic mixtures in a nanotube. Colloids Surf, A 610:125905
41. Duval JFL, Ohshima H (2006) Electrophoresis of diffuse soft particles. Langmuir 22(8):3533–3546
42. Israelachvili JN (2011) Intermolecular and surface forces. Academic press
43. Hasted JB, Ritson DM, Collie CH (1948) Dielectric properties of aqueous ionic solutions. Parts I and II. J Chem Phys 16(1):1–21
44. Li H, Lu B (2014) An ionic concentration and size dependent dielectric permittivity Poisson-Boltzmann model for biomolecular solvation studies. J Chem Phys 141(2):07B609_1
45. Hess B, Holm C, van der Vegt N (2006) Modeling multibody effects in ionic solutions with a concentration dependent dielectric permittivity. Phys Rev Lett 96(14):147801
46. Biesheuvel PM, Leermakers FAM, Stuart MAC (2006) Self-consistent field theory of protein adsorption in a non-gaussian polyelectrolyte brush. Phys Rev E 73(1):011802
47. Chakraborty J, Chakraborty S (2013) Influence of hydrophobic effects on streaming potential. Phys Rev E 88(4):043007
48. Bandopadhyay A, Chakraborty S (2012) Combined effects of interfacial permittivity variations and finite ionic sizes on streaming potentials in nanochannels. Langmuir 28(50):17552–17563
49. Chakraborty S, Das S (2008) Streaming-field-induced convective transport and its influence on the electroviscous effects in narrow fluidic confinement beyond the debye-hückel limit. Phys Rev E 77(3):037303
50. Chakraborty J, Ray S, Chakraborty S (2012) Role of streaming potential on pulsating mass flow rate control in combined electroosmotic and pressure-driven microfluidic devices. Electrophoresis 33(3):419–425
51. Chen G, Das S (2015) Streaming potential and electroviscous effects in soft nanochannels beyond debye-hückel linearization. J Colloid Interface Sci 445:357–363
52. Leonard BP (1979) A stable and accurate convective modelling procedure based on quadratic upstream interpolation. Comput Methods Appl Mech Eng 19(1):59–98
53. Patankar SV (1980) Numerical heat transfer and fluid flow. Hemisphere, Washington DC
54. Bowen WR, Cao X (1998) Electrokinetic effects in membrane pores and the determination of zeta-potential. J Membr Sci 140(2):267–273
55. Bhattacharyya S, De S (2016) Influence of rigid core permittivity and double layer polarization on the electrophoresis of a soft particle: A numerical study. Phys Fluids 28(1):012001
56. Stein D, Kruithof M, Dekker C (2004) Surface-charge-governed ion transport in nanofluidic channels. Phys Rev Lett 93(3):035901
57. Karnik R, Fan R, Yue M, Li D, Yang P, Majumdar A (2005) Electrostatic control of ions and molecules in nanofluidic transistors. Nano Lett 5(5):943–948
58. Prakash S, Zambrano HA, Rangharajan KK, Rosenthal-Kim E, Vasquez N, Conlisk A (2016) Electrokinetic transport of monovalent and divalent cations in silica nanochannels. Microfluid Nanofluid 20(1):8
59. Buren M, Jian Y, Zhao Y, Chang L (2018) Electroviscous effect and electrokinetic energy conversion in time periodic pressure-driven flow through a parallel-plate nanochannel with surface charge-dependent slip. J Phys D: Appl Phys 51(20):205601
60. Ohshima H (2016) An approximate analytic solution to the modified poisson-boltzmann equation: effects of ionic size. Colloid Polym Sci 294(12):2121–2125